Structure and growth of butane films adsorbed on graphite

K. W. Herwig, J. C. Newton,* and H. Taub
Department of Physics and Astronomy and University of Missouri Research Reactor Facility, University of Missouri–Columbia, Columbia, Missouri 65211
(Received 25 February 1994; revised manuscript received 18 July 1994)

The structure of deuterated *n*-butane [$CD_3(CD_2)_2CD_3$] adsorbed on the (0001) surfaces of an exfoliated graphite substrate has been investigated by elastic neutron diffraction. The aim of this study was to elucidate the effect of steric properties, particularly the rodlike shape of the molecule, on both the monolayer and multilayer film structure. Our principal findings are as follows: (1) The solid monolayer has a rectangular unit cell commensurate with the graphite lattice in one direction ($2\sqrt{3}\times\infty$). Profile analysis of the monolayer diffraction pattern shows an improved fit with two molecules in the unit cell arranged in a herringbone (HB) pattern rather than the rectangular-centered structure originally proposed. The HB structure also yields a lower potential energy calculated for a monolayer cluster. (2) The growth mode of the film is "quasiepitaxial" at low temperature consisting of the following steps: (a) adsorption of the crystalline monolayer, (b) adsorption of a disordered second layer and compression of the monolayer, (c) onset of preferentially oriented bulk growth with continued adsorption of disordered material, (d) bilayer crystallization, and (e) reentrant growth of preferentially oriented bulk particles and disordered material. (3) A Rietveld profile analysis of the diffraction pattern obtained at a coverage of six layers is consistent with the (100) plane of the bulk butane monoclinic phase parallel to the graphite surface. (4) For coverages of two to three layers, there is evidence of a wetting transition at ~ 133 K, about 2 K below the bulk melting point. Both the monolayer and bulk Bragg peaks disappear and are replaced by a diffraction pattern characteristic of a liquid film with a high degree of short-range order. It is suggested that the butane molecule's steric properties are responsible for the incomplete wetting of the film as well as for the preferential orientation of the bulk phase. Our quasiepitaxial growth model for butane is similar to one proposed previously for nitrogen films on graphite. After comparing the structure and growth of the two films, we suggest that it may apply to a number of other physisorbed films composed of rod-shaped molecules having a larger aspect ratio than butane.

I. INTRODUCTION

Molecular steric properties can strongly affect the structure and phase transitions of films physisorbed on a solid substrate. Previous work with linear-chain hydrocarbon molecules adsorbed on the basal-plane surfaces of graphite has shown that the molecular size, shape, symmetry, and flexibility can play an important role in determining the monolayer structure[1] and the nature of its melting transition.[2] These steric effects are not only of fundamental interest in understanding the intermolecular and molecule-substrate interactions, they are also of technological importance in applications such as lubrication and adhesion where hydrocarbon molecules are confined between two solid surfaces.[3]

The focus of the present neutron-diffraction study was to investigate the solid multilayer structure of a film consisting of one of the shorter alkane molecules, *n*-butane [$CH_3(CH_2)_2CH_3$]. Of particular interest to us was the question of how the rodlike shape of a molecule might influence the growth of the multilayer film. For example, if the molecular orientational order in the monolayer differs from that of all planes of the bulk crystal, one might expect either a restructuring of the bottom layer when more layers are added or a structural discontinuity between lower and higher layers.[4,5] If neither of these alternatives is realized, the resulting orientational "frustration" may reduce the ultimate film thickness. This type of orientational mismatch in molecular films is analogous to the lattice mismatch occurring in films of spherical molecules when, due to strong substrate binding, the monolayer is compressed to a lattice constant smaller than that of the bulk crystal.[5–8]

We chose *n*-butane for our study because, as will be discussed below, the structure of its solid monolayer phase on the graphite (0001) surface resembles[9] that of the close-packed (100) plane of the low-temperature bulk monoclinic phase.[10] This similarity suggested to us that orientational frustration might be minimized in this system, enabling epitaxial growth of the butane film. On the other hand, butane's rodlike shape results in a strong preference to orient with its long axis parallel to the graphite surface whereas this axis tilts out of the densest-packed plane of the bulk phase. If this source of orientational frustration were important in butane films, one might expect it to be so in a large number of films of other rod-shaped molecules.

Neutron diffraction, like x-ray scattering, is well suited to investigating multilayer film structures due to the penetration of the probe compared to that achieved in electron and atom diffraction. The disadvantage of the weak interaction of the neutron with the film is the necessity of using a high-surface-area polycrystalline substrate with the attendant capillary condensation of bulk materi-

al.[4,11] However, we shall see that bulk nucleation of butane in our sample occurs at a coverage less than two layers where the effects of capillary condensation should be greatly reduced.

As discussed above, knowledge of the molecular orientational order in the monolayer can be critical to understanding the multilayer film structure. In the case of butane, an earlier investigation by Trott and co-workers[12,13] proposed a rectangular-centered (RC) unit cell for a monolayer on the graphite (0001) surface. Although the diffraction profile calculated for this cell gave reasonable agreement with the measured pattern, the authors noted that the orientation of the butane molecule was energetically unfavorable. In addition, diffraction data and potential-energy calculations for both shorter (ethane) and longer (hexane) *n*-alkanes physisorbed on graphite were consistent with a herringbone (HB) unit cell.[1,9] For these reasons, the previously published structure of butane[13] appeared anomalous and prompted the present effort to investigate the possibility of an HB structure for the butane monolayer.

This paper is organized as follows. Section II provides some experimental details, which are followed by a presentation of the observed neutron-diffraction data as a function of coverage and temperature in Sec. III. These results are discussed in Sec. IV and used to develop a qualitative model describing the "quasiepitaxial" growth of the butane film on the graphite basal-plane surface. A brief summary and conclusions are presented in Sec. V.

II. EXPERIMENTAL DESCRIPTION

The neutron-diffraction patterns were obtained using the two-axis diffractometer located at C-port of the University of Missouri Research Reactor. This diffractometer is equipped with a five-counter multidetector data-acquisition system.[14] It was operated at a wavelength of 1.278 Å selected by a copper (220) monochromator having a mosaic spread of 0.75° full width at half maximum. Collimation was 0.92°, 1.2°, and 0.33° before the monochromator, between the monochromator and the sample, and between the sample and the detectors, respectively. As in previous experiments,[15] diffraction was performed in a transmission geometry.

Deuterated butane (98% n-C_4D_{10}) was used as the adsorbate in order to reduce incoherent scattering from hydrogen. The comparable coherent cross sections of C and D result in a monolayer structure factor for neutrons, which is more sensitive to molecular orientation than for x-rays.[1]

The sample cell, cryostat, and substrate surface-area calibration procedure were the same as that used previously.[15] The substrate consisted of a stack of 40 disks of an exfoliated graphite, Papyex,[16] having a mass of 51 g and aligned with the disk planes parallel to the scattering vector **Q**. Thermal gradients between the top and bottom of the sample cell were determined to be less than 2 K near the melting temperature of bulk butane, 135 K,[17] with the bottom of the sample cell being cooler. In the temperature range of 108–133 K, the temperature accuracy and stability was ±0.1 K. When changing coverage, precautions were taken to ensure that all of the added butane gas reached the graphite substrate and did not condense in the capillary tubing. The cryostat was first warmed to room temperature and the desired gas was then admitted to the cooling sample cell through a heated capillary tube. Throughout this paper, the adsorbed volume of butane is expressed in coverage units θ where $\theta=1$ corresponds to the number of butane molecules in the complete monolayer (32.7 Å^2/molecule as discussed below).

Diffraction patterns were measured at 14 butane coverages ranging from $\theta=0.9$ to 6.0 at a sample temperature of 11 K. In addition, the temperature dependence of the patterns was investigated at coverages of $\theta=2.2$, 3.1, and 6.0. Background diffraction patterns from the bare graphite substrate were obtained at two temperatures, 11 and 128 K. For each diffraction pattern taken with the adsorbate present, the background pattern closest in temperature was subtracted. Typically, a monolayer diffraction pattern would take ~50 h to collect (38 min per point) with ~15 000 counts in the most intense Bragg peak after background subtraction. Progressively shorter data collection times were used at higher coverages. The 0.9 monolayer diffraction data were analyzed using a profile-analysis technique, which has been described elsewhere.[12,13]

III. RESULTS

A. Monolayer structure

A neutron-diffraction pattern was obtained at a butane coverage of $\theta=0.9$ and a temperature of 11 K as shown in Fig. 1. This pattern is in reasonable agreement with those measured previously.[9,12,13,18] The solid curve in Fig. 1 shows the best fit that could be obtained with an HB model in which glide-line symmetry was imposed parallel to both sides of the rectangular unit cell. The fit corresponds to the unit cell depicted in Fig. 2(a), which has lattice constants $a=8.52$ Å and $b=7.68$ Å and the azimuthal angle $\psi=15°$. As is the case with monolayer n-hexane on graphite,[1,9] both molecules in the unit cell have their carbon skeletal plane parallel to the surface ($\alpha=0$, $\beta=0$). The fit yields an R factor (as defined in Ref. 19) of 27% compared with a value of 35% obtained for the RC model.

In comparing the earlier RC model[12,13] with the HB model of the butane monolayer in Fig. 2(a), we see that they have the same dimensions of the rectangular unit cell and both have the long axis of the molecules nearly parallel to the short side of the cell. The structures differ in that the two molecules in the HB unit cell have opposite sense azimuthal rotations from the **b** direction by an angle $\psi=15°$, while in the RC model these rotations have the same sense. The models also differ in the orientation of the carbon skeletal plane with respect to the graphite surface. In the RC model, both molecules in the cell are tilted at an angle $\alpha=30°$ to the surface [see Fig. 2(b)], whereas in the HB model the carbon skeletal plane is parallel to the surface but with the α angles of the molecules differing by 180°.

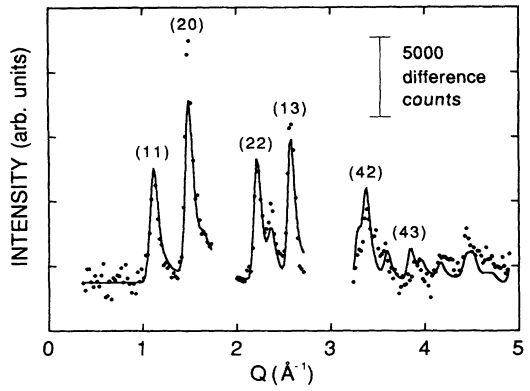

FIG. 1. Diffraction pattern of 0.9 layer of butane on Papyex at 11 K after the substrate scattering has been subtracted. The solid line is the best fit to a HB model as discussed in the text. Gaps in the measured diffraction pattern appear in Q ranges of intense scattering from the graphite substrate.

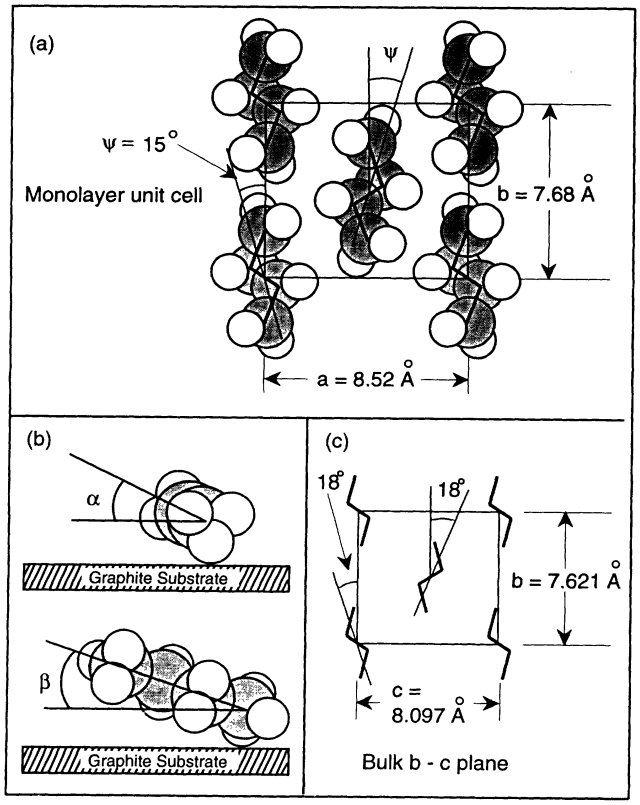

FIG. 2. Models of the monolayer and bulk butane structures. (a) Projection of the HB monolayer structure on the graphite (0001) surface. For clarity, the van der Waals radii of individual atoms have been reduced by approximately 50%. (b) Diagrams defining the out-of-plane orientational parameters α and β: view along the long axis of the molecule (top panel) and perpendicular to the long axis (lower panel). (c) Projection of the low-temperature monoclinic structure of bulk butane on the (100) plane. The carbon skeleton of the butane molecules is represented by a thick solid line.

As a test of the structure inferred experimentally, we have calculated the potential energies of an 18-molecule monolayer butane cluster on a smooth graphite substrate (no corrugation) for both the HB and RC models.[9] Molecule-substrate and intermolecular interactions were calculated using atom-atom potentials of the Lennard-Jones type with parameters fitted to Buckingham potentials proposed by Kitaigorodskii.[13,20] To obtain the molecule-substrate interaction, carbon-substrate and hydrogen-substrate potentials were constructed as a function of adatom height by averaging over different lateral positions of the adatom. In minimizing the cluster potential energy, the lattice parameters of the rectangular unit cell and the molecular angle α were held fixed at their experimentally determined values. Only the azimuthal angle ψ and the height of the molecule above the surface were allowed to vary. The results of these calculations, summarized in Table I, show that the HB model has significantly lower intermolecular and molecule-substrate energies than those of the RC model. Together with the improved R factor in the fit to the monolayer diffraction pattern, these results demonstrate the HB model to be a better solution to the butane monolayer structure than the previous RC model.

It is also of interest to compare the HB monolayer structure with that of bulk butane as recently determined using neutron diffraction by Refson and Pawley.[10] One sees in Fig. 2(c) that the molecules in the (100) plane of the low-temperature monoclinic bulk phase have nearly the same azimuthal orientation as in the HB monolayer. However, the molecules in the bulk structure are tilted out of the (100) plane by $\sim 22°$. Comparing lattice constants, the monolayer value of b is only $\sim 1\%$ larger than in bulk, whereas a in the monolayer is expanded $\sim 5\%$ with respect to c in the bulk. The monolayer expansion in the a direction may be caused by the lateral forces of registry since the monolayer is commensurate with the graphite substrate in this direction: $a = 8.52$ Å $= 2\sqrt{3}a_g$ where $a_g = 2.46$ Å is the lattice constant of the graphite basal plane. The structural similarity of the monolayer and the bulk (100) plane suggested that epitaxial growth of a multilayer butane film could be possible.

TABLE I. Results of potential-energy calculations described in the text for the RC and HB models using an 18-molecule monolayer butane cluster adsorbed on the graphite (0001) surface. Lattice constants of the rectangular unit cell [see Fig. 2(a)] and the molecule angle α [Fig. 2(b)] have been fixed at the experimentally determined values: $a = 8.52$ Å, $b = 7.68$ Å, and $\alpha = 0$ (HB model) and $\alpha = 30°$ (RC model). Energies are in cal/mole. The calculated value for the azimuthal angle ψ [see Fig. 2(a)] is given in degrees and the height z of the molecular center-of-mass in angstroms.

Model	Molecule-substrate energy	Molecule-molecule energy	Total energy	ψ	z
RC	-7.1×10^3	-1.8×10^3	-8.9×10^3	10	3.95
HB	-9.1×10^3	-2.9×10^3	-12.0×10^3	15	3.65

B. Coverage dependence of the butane diffraction patterns

The coverage dependence of the butane film diffraction patterns at a temperature of 11 K is shown in Fig. 3. It should be emphasized that the coverage units only indicate the amount of butane in the sample cell, not the number of solid butane layers. In agreement with earlier measurements,[9] little change is seen in the diffraction patterns until the coverage reaches $\theta=1.9$ where excess intensity (over that of the monolayer pattern) first appears. This extra intensity evolves with increasing coverage into intense, sharp peaks in the $\theta=6.0$ scan, which can be indexed according to the low-temperature monoclinic structure of bulk butane[10] as labeled at the top of Fig. 3.

To determine the onset coverage for bulk nucleation, we have plotted in Fig. 4(a) the coverage dependence of the integrated diffracted intensity in the region near the (051) bulk reflection ($4.10\ \text{Å}^{-1}<Q<4.35\ \text{Å}^{-1}$). This region is free of monolayer Bragg peaks as well as those of a bilayer (see Sec. IV B). The intensity begins to rise at $\theta=1.7$, consistent with bulk nucleation at this coverage. Analysis of the temperature dependence of the diffraction patterns presented in Sec. IV B is also consistent with bulk nucleation at $\theta\approx 2$. In the coverage range $2.6<\theta<3.8$, the bulk (051) peak intensity levels off followed by a slower linear increase for $\theta>3.8$. The question of where this bulk material is growing will be discussed in Sec. IV.

As a measure of the amount of disordered material in the cell, we have also monitored the diffuse intensity in a Q range below the first Bragg peak of either the monolayer or bulk butane.[21] The integrated intensity in the range $0.4\ \text{Å}^{-1}<Q<1.0\ \text{Å}^{-1}$ is plotted as a function of coverage in Fig. 4(b). Interestingly, this diffuse intensity has qualitatively the same coverage dependence as that of the bulk peak in Fig. 4(a). It levels off in the coverage range $2.5<\theta<3.4$ and has a linear increase at lower and higher coverages with a smaller slope at higher θ.

Another change that occurs in the diffraction patterns as the butane coverage increases is a shift to higher Q in the peak at the monolayer (22) position. This shift does not occur for the (20) peak, which is also relatively well separated from bulk reflections. We interpret this behavior as indicating a uniaxial compression of the monolayer along the **b** direction [see Fig. 2(a)] with increasing coverage. Figure 4(c) shows the coverage depen-

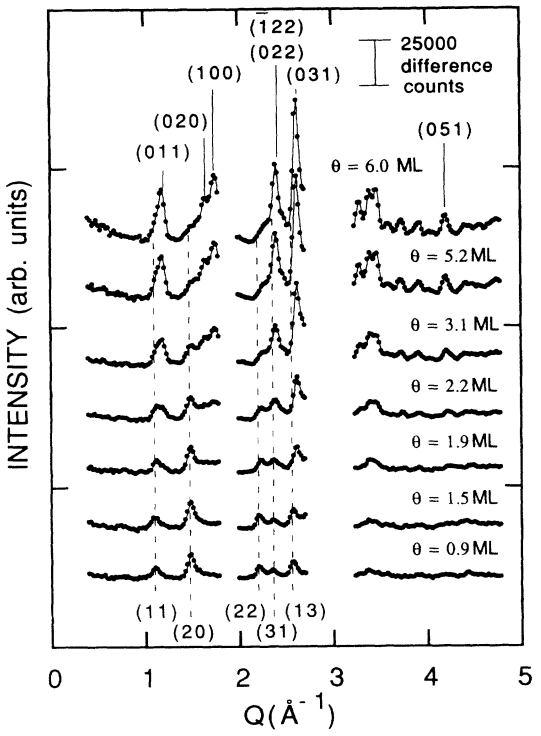

FIG. 3. Coverage dependence of the butane film diffraction patterns at a temperature of 11 K. Solid lines connecting the points are guides to the eye. The vertical dashed lines indicate the position of prominent monolayer Bragg peaks labeled at the bottom of the figure. The strongest Bragg peaks of bulk butane are labeled at the top of the figure according to the monoclinic structure determined in Ref. 10. Gaps in the data occur in Q ranges of intense scattering from the graphite substrate.

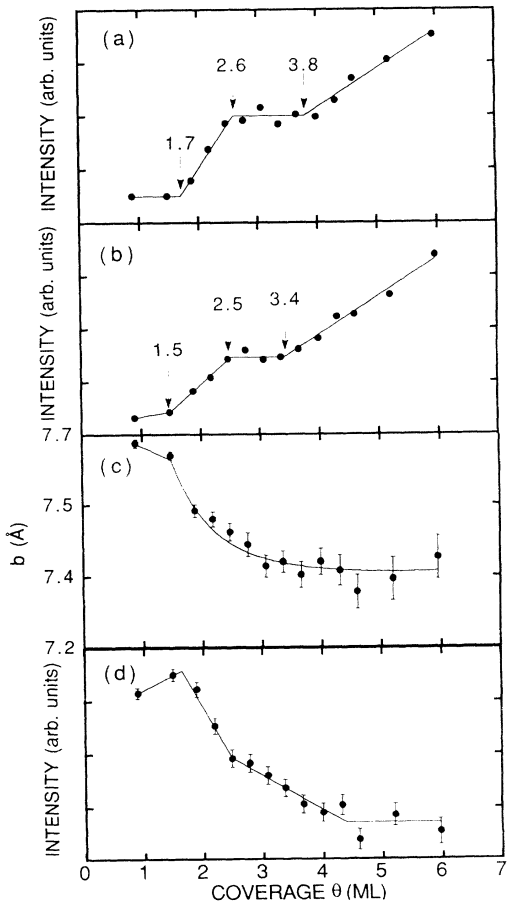

FIG. 4. Analysis of the coverage dependence of the butane diffraction patterns in Fig. 3. (a) Integrated intensity of the bulk (051) Bragg peak; (b) integrated diffuse intensity in the range $0.4\ \text{Å}^{-1}<Q<1.0\ \text{Å}^{-1}$; (c) the b lattice constant of the monolayer as determined from the (22) Bragg peak position; and (d) the monolayer (20) peak intensity. In each case, the solid lines are guides to the eye.

dence of the b lattice constant as determined from the shift of the (22) peak. A maximum compression of $\sim 4\%$ is reached at a coverage $\theta \approx 3.5$ where $b = 7.38$ Å $= 3a_g$. Thus, the uniaxial compression proceeds until the rectangular unit cell of the film is completely commensurate $(2\sqrt{3} \times 3)$ with the graphite (0001) surface.

Although the monolayer (20) peak does not shift in position, one sees in Fig. 4(d) that its intensity weakens in roughly the same coverage range in which the uniaxial compression of the film occurs. This behavior may be related to crystallization of the bilayer as will be discussed in Sec. IV B.

C. Temperature dependence of the diffraction patterns above monolayer completion

Figure 5 shows the temperature dependence of the diffraction patterns at a coverage of $\theta = 2.2$. A similar behavior was observed at $\theta = 3.1$. As discussed above, the low-temperature patterns at these coverages contain sharp peaks attributed to monolayer and bulk butane. These peaks disappear between 128 and 133 K and are replaced by a single broad peak centered on the monolayer (20) position. This implies that, at these higher coverages, the monolayer is melting at least 12 K above the 116 K melting point observed at a coverage $\theta = 0.8$.[2,12,13]

Recent heat-capacity experiments have investigated the melting of butane films adsorbed on graphite.[22,23] They show that the monolayer melting point is nearly constant at 113 K for coverages $\theta \leq 0.83$ and then increases rapidly to 133 K at a coverage $\theta = 1.08$. By $\theta \sim 2$, it is within 1 K of the bulk melting point at 134.8 K. The different submonolayer melting points of 112.5 and 116 K as determined from heat capacity and neutron measurements, respectively, could be due to errors in either coverage or temperature determination in the two experiments. At higher coverages, the 12 K increase in the monolayer melting point inferred from the neutron-diffraction patterns is somewhat less than would be anticipated from the heat-capacity results. Further heat-capacity measurements are in progress to try to resolve these discrepancies.[23]

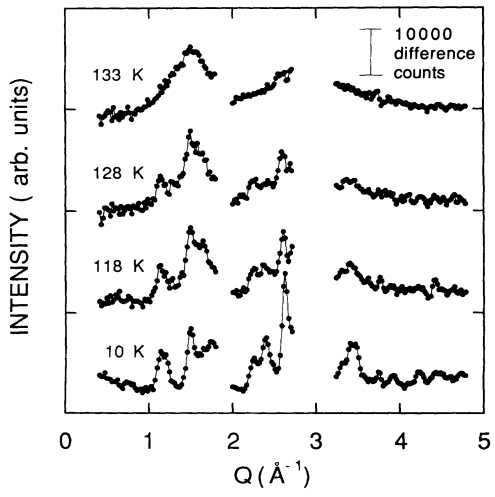

FIG. 5. Temperature dependence of the diffraction patterns at a coverage $\theta = 2.2$.

The interpretation of the disappearance of bulk peaks by 133 or 1.8 K below the bulk butane melting point will be discussed in Sec. IV E. Here, we only remark that it cannot be explained by the small temperature gradient (< 2 K) across the sample, since the temperatures reported above refer to the warmest part of the sample.

IV. DISCUSSION

A. Monolayer structure

The analysis of the butane monolayer structure presented above resolves the apparent anomaly[12,13] with respect to that of other n-alkane monolayers adsorbed on the graphite (0001) surface. The structure depicted in Fig. 2(a) is similar to that of ethane[1] and n-hexane,[1,9,24] having a rectangular unit cell with a two-sublattice herringbone arrangement of the molecules. As for n-hexane, the carbon skeletal plane of the n-butane molecules is parallel to the graphite surface in agreement with potential-energy calculations. The butane film structure differs from that of ethane and hexane in that at monolayer completion the unit cell is commensurate with the substrate in only one direction. However, we have seen that the film approaches complete commensurability $(2\sqrt{3} \times 3)$ with the graphite (0001) surface at higher coverages. Thus, butane joins a large family of nonspherical molecules, which exhibit a rectangular commensurate herringbone phase on graphite.[1]

B. Evidence for a crystalline bilayer

We have analyzed the 11 K diffraction patterns in Fig. 3 for evidence of a crystalline film thicker than a monolayer. This effort included unsuccessful attempts to find a crystalline bilayer model that would fit the patterns at coverages $\theta = 1.9$ and 2.2. Attempts at higher coverages were hampered by the presence of bulk Bragg peaks in the diffraction patterns. Nevertheless, the results of recent heat-capacity experiments[23] have led us to reconsider the possibility of a crystalline bilayer. These show a sharp heat capacity peak at a temperature of ~ 114 K for coverages $\theta \geq 2.5$, which is most easily interpreted as due to melting of a second butane layer.

At this point, we have only indirect evidence to support crystallization of a butane bilayer. In the coverage range $1.5 < \theta < 3.5$, we have interpreted the diffraction patterns as indicating a uniaxial compression of the film in the direction of the monolayer **b** lattice vector. However, it is difficult to understand how compression of the film could occur at such high coverages if only the first layer were crystalline. Even in cases of molecular orientational reordering, compression of a physisorbed monolayer is usually complete by a coverage $\theta \sim 1.5$.[12,15] Film compression above this coverage range might be explained by a tilting of the butane molecules away from the surface, which results in the first two layers locking together to form a bilayer crystal.[25] It is interesting to note that bilayer crystallization accompanied by some molecular reorientation is also believed to occur at low

temperature for N_2 adsorbed on graphite in about the same coverage range.[15] As in the case of N_2, the butane bilayer crystallization would occur after disordered molecules adsorb in a third layer.

Further evidence of bilayer crystallization comes from the coverage dependence of the monolayer (20) Bragg peak intensity plotted in Fig. 4(d). For coverages $1<\theta<1.5$, there is a slight increase in intensity as the monolayer completes. However, at higher coverages the (20) peak intensity falls monotonically at about the same rate at which the compression is occurring in the monolayer b lattice constant. This could be explained by a different structure factor for this peak in the bilayer than in the monolayer.

Crystallization of a butane bilayer could also explain the leveling off in the intensity of the bulk and diffuse contributions to the scattered intensity observed in the coverage range $2.5<\theta<3.4$ [see Figs. 4(a) and 4(b)]. This behavior is consistent with the second layer of the film crystallizing while additional molecules replenish the amount of disordered material. The quantity of bulk material in the cell would remain constant in this process.

C. Preferential orientation in the bulk phase

Our results demonstrate that butane on graphite is an extreme example of incomplete wetting in that, as coverage is increased at low temperature, only one or possibly two layers crystallize prior to bulk nucleation. Despite the structural similarity noted in Sec. I between the monolayer and bulk (100) plane (see Fig. 2), there is apparently sufficient lattice and orientational mismatch to limit film growth. The greatest source of orientational frustration appears to be the difference in the "out-of-plane" tilt angles of the monolayer and bulk (100) plane defined in Fig. 2(b). These angles have the values $\alpha=8°$ and $\beta=22°$ (Ref. 10) for the bulk (100) plane whereas both are zero in the solid monolayer. We also note that the lattice mismatch between the film and the bulk (100) plane worsens at higher coverage. Although the 5% misfit between the film a lattice constant and the bulk c lattice constant is coverage independent, this is not the case for the misfit of the b lattice constant of the film and bulk. The value of b in the monolayer is only $\sim 1\%$ *larger* than in bulk; but by $\theta=2.5$, at the onset of bilayer crystallization, it has compressed to a value 3% *smaller* than in the bulk.

While the growth of a monolithic film appears to end with the completion of bilayer crystallization at a coverage $\theta\approx 3.4$, the structure of the bulk butane, which grows at higher coverages appears, nevertheless, to be influenced by the substrate proximity. We have performed a Rietveld profile analysis[19] of a high-coverage diffraction pattern, which demonstrates that the bulk butane present has a preferential orientation with respect to the graphite substrate. In Fig. 6, the difference between the diffraction patterns observed at coverages of $\theta=6.0$ and $\theta=3.4$ has been plotted (filled circles). This difference pattern is dominated by scattering from the bulk butane, which grows in the cell at coverages $\theta\geq 3.4$ [see Fig. 4(a)].[26] It is compared with two Rietveld profiles calculated for polycrystalline bulk butane using the GSAS computer code developed by Larson and Von Dreele.[27] Both calculated profiles assume the structural parameters of the low-temperature monoclinic phase found by Refson and Pawley[10] but differ in the orientational distribution assumed for the bulk crystallites. The dashed curve in Fig. 6 is calculated for an isotropic powder. It shows the combined intensity of the overlapping $(\bar{1}22)$ and (022) peaks to be greater than that of the (031) reflection. This differs from the observed diffraction pattern where the (031) peak is the strongest observed.

A better fit to the bulk diffraction pattern in Fig. 6 can be obtained by assuming preferential orientation of the bulk crystallites with respect to the scattering plane. Since the Papyex disks composing the substrate are aligned parallel to the scattering plane and the graphite particles within the disks have their (0001) plane preferentially oriented parallel to the plane of the disk,[28] this assumption is tantamount to the bulk butane crystallites having a preferred orientation with respect to the graphite (0001) surfaces.

Preferred orientation is introduced in the GSAS code using the formalism of Dollase[29] and March.[30] For simplicity, a single preferred crystallographic axis was assumed. The free parameters in the model were the direction of the preferred axis with respect to the scattering plane, the volume fraction of preferred crystallites, and a coefficient characterizing the strength of the preferred orientation. This coefficient can be related to the width of the angular distribution of the preferred axis with respect to the scattering plane.

Guided by the similarity of the bulk (100) plane to that of the monolayer (see Fig. 2), the (100) plane normal was chosen as the preferred axis and assumed to have a nearly Gaussian distribution about the normal to the scattering plane. The Rietveld profile, which gave the best fit to the bulk pattern under these constraints, is shown as the solid curve in Fig. 6. It yields a 50% volume fraction of

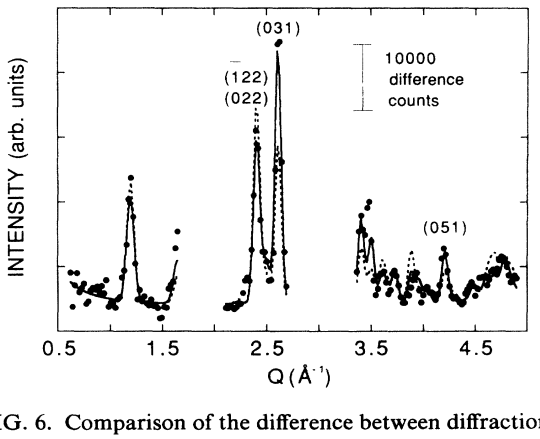

FIG. 6. Comparison of the difference between diffraction patterns observed at coverages of $\theta=6.0$ and $\theta=3.4$ at a temperature of 11 K (filled circles) with Rietveld profiles calculated for an isotropic distribution of bulk crystallites (dashed curve) and for preferential orientation of the (100) plane of the bulk crystallites parallel to the scattering plane (solid curve) as discussed in the text. Note that subtraction of the observed diffraction pattern at a coverage $\theta=3.4$ removes most of the scattering from the butane film.

preferentially oriented bulk crystallites having a distribution width of 28° [full width at half maximum (FWHM)] with the remaining 50% volume fraction isotropically oriented. The fit is clearly much better than that obtained assuming a completely isotropic bulk powder (dashed curve).

If all the bulk crystallites had a (100) plane parallel to a graphite surface, the width of the angular distribution of bulk butane (100) axes with respect to the scattering plane should be the same as that of the graphite c axes. The FWHM $=28°$ obtained from the fit in Fig. 6 is in good agreement with the c-axis mosaic spread of 30° measured for an exfoliated graphite similar to Papyex.[28] Better agreement should not be expected since the graphite mosaic measures the mass-weighted distribution of c axes rather than the angular distribution weighted by the particle surface area. The inferred 50% volume fraction of isotropically oriented bulk crystallites may result from capillary-condensed material or from oriented bulk crystallites on the basal-plane surfaces of small, randomly oriented graphite particles.

Although assuming preferential orientation of the bulk butane (100) plane parallel to the graphite surface improves the fit to the bulk pattern in Fig. 6, it is difficult to exclude the possibility of another orientational distribution yielding as good a fit. However, we next show that the assumed orientational distribution is also consistent with the temperature dependence of the diffraction patterns observed at coverages $\theta \geq 2.2$.

Our analysis exploits the structural transformation, which bulk monoclinic butane undergoes upon heating. At 108 K, a first-order phase transition occurs from a fully ordered structure to a plastic phase in which the molecules are rotationally disordered about their long axis.[31] In their neutron-diffraction experiments on bulk butane powders, Refson and Pawley determined the structure of the plastic phase at 120 K as well as that of the low-temperature phase at 90 K.[10] The two structures are sufficiently dissimilar that we are able to use the difference in their respective diffraction patterns as a test for the presence of bulk material. Assuming the structural parameters of Ref. 10, we have calculated the Rietveld diffraction profiles of both bulk phases. The difference between these calculated profiles (high temperature minus low temperature) after folding with our instrumental resolution function is plotted in Fig. 7(a) for an isotropic bulk powder and in Fig. 7(b) assuming the orientational distribution of bulk crystallites inferred from the fit to the bulk pattern in Fig. 6. A dip in these difference profiles corresponds to a peak in the low-temperature diffraction pattern, which is not present in the high-temperature phase, whereas a peak corresponds to a reflection in the high-temperature pattern, which is absent below the transition.

In Fig. 7, the calculated difference profiles are compared to the difference between observed diffraction patterns above and below the transition temperature at three different butane coverages. It is evident that the difference profile calculated assuming preferential orientation in the bulk [Fig. 7(b)] rather than that of an isotropic powder [Fig. 7(a)] gives better agreement with the observed difference patterns [Figs. 7(c)–7(e)]. In the isotropic calculation, the peak and dip in the difference profile near $Q=1.6$ Å^{-1} are much larger than observed and the two dips near $Q=1.6$ Å^{-1} have the wrong relative intensity. Thus, the qualitative agreement between the calculated difference profile in Fig. 7(b) and the observed difference patterns not only supports the presence of bulk butane in the cell at coverages as low as $\theta=2.2$ but also is consistent with the assumed preferential orientation of the bulk (100) planes parallel to the graphite surface. Presumably, the poorer agreement with the calculated difference profile at lower coverages is due to finite-size effects, which broaden the bulk Bragg peaks.[32]

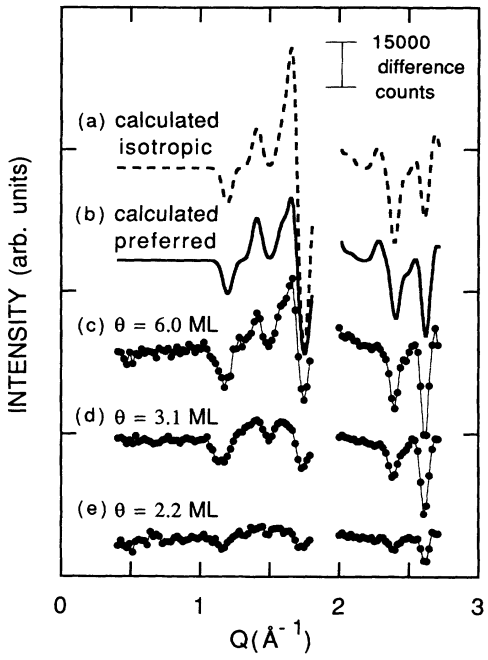

FIG. 7. Evidence of the presence of bulk butane from the temperature dependence of the diffraction patterns. (a) The *difference* between Rietveld profiles calculated for the high-temperature plastic phase of bulk butane and the orientationally ordered low-temperature phase assuming an isotropic powder and after folding with the resolution function for the diffractometer used in the present experiments. (b) Same as for (a) except preferential orientation of the bulk material is assumed as for the solid curve in Fig. 6. In the bottom part of the figure are the difference between diffraction patterns observed above and below the bulk crystalline-to-plastic transition temperature of 108 K for three different coverages: (c) $\theta=6.0$; (d) $\theta=3.1$; and (e) $\theta=2.2$.

D. Coverage dependence of the bulk and diffuse scattering

It is interesting to consider why bulk growth begins at a coverage $\theta=1.7$, levels off during bilayer crystallization, and then resumes at a slower rate at coverages $\theta \geq 3.8$ as measured by the bulk (051) peak intensity in Fig. 4(a). There are several reasons why we believe it unlikely that the bulk butane, which initially appears at $\theta=1.7$, results from capillary condensation. First, this is a lower coverage than at which capillary condensation

occurs for other adsorbates on exfoliated graphite. In the case of N_2 adsorption on the *same* Papyex substrate, bulk did not appear until a coverage equivalent to 3.7 layers.[16] This is about the same coverage at which bulk appeared in the adsorption of Ar on a vermicular graphite substrate.[11] Also, Morishige *et al.*[33] report the appearance of bulk Xe just above bilayer formation on a loosely packed form of exfoliated graphite rather than below bilayer crystallization as we have observed for butane.

Second, it is difficult to understand why, if the bulk appearing at $\theta=1.7$ is capillary condensed, its growth should level off in the coverage range $2.6<\theta<3.8$ [see Fig. 4(a)]. Previous experiments[11,15,33] show a monotonic growth in bulk material after the onset of capillary condensation. From this comparison, we believe it is more likely that capillary condensation of butane is occurring at coverages above $\theta=3.8$ at which a roughly linear increase of bulk resumes. We emphasize that this is about the same coverage at which bulk N_2 first appeared on the same Papyex substrate.

Third, we would expect capillary-condensed bulk particles to be isotropically oriented, since these do not nucleate on the graphite basal-plane surfaces but at particle edges and in pores having no preferred orientation. However, the analysis of the difference patterns in Fig. 7 indicates that, even at coverages as low as $\theta=2.2$, the bulk butane in the sample is preferentially oriented. That is, the observed difference pattern in Fig. 7(e) is qualitatively closer in shape to the difference profile calculated assuming preferred orientation [Fig. 7(b)] than for an isotropic powder [Fig. 7(a)].

There is further evidence to support growth of preferentially oriented bulk material at coverages $\theta\approx2.2$ with capillary condensation of isotropically oriented bulk particles delayed to higher converges. In Fig. 4(a), we find a larger slope in the bulk (051) peak intensity in the coverage range $1.7<\theta<2.6$ than for $\theta>3.8$. Since the (051) peak intensity is sensitive to the amount of preferred orientation in the bulk (compare solid and dashed curves in Fig. 6), we would expect it to increase more rapidly with coverage when there is growth of only preferentially oriented bulk particles.

We have interpreted the low-Q diffuse intensity [Fig. 4(b)] as measuring the amount of disordered material in the sample cell. Even below a coverage $\theta=1.5$ at which this diffuse intensity is observed to rise, there is evidence of disordered material in the cell. The monolayer diffraction pattern is essentially unchanged in the coverage range $\theta=1.0-1.9$; whereas, if the positions of butane molecules in the second layer were correlated with those of the first layer, we would expect some modulation of the monolayer Bragg peak intensities. Therefore, we suggest that, upon monolayer completion, molecules adsorb in a disordered second layer, which mitigates the orientational and lattice mismatch between the crystalline monolayer and the (100) planes of the bulk particles beginning to nucleate at a coverage $\theta\approx1.7$.

The growth rate of disordered material in the cell appears to increase at $\theta\approx1.5$, about the same coverage as the onset of bulk nucleation and of monolayer compression. There is a linear increase in the low-Q diffuse intensity for coverages from $\theta=1.5-2.5$ [see Fig. 4(b)]. We suggest that the disordered material continues to accumulate at the monolayer-bulk interface in this coverage range, causing the uniaxial monolayer compression [see Fig. 4(c)] and subsequent bilayer crystallization. It seems less plausible to us that the monolayer compression could result from bulk crystallites, which incompletely cover the area occupied by the monolayer.[32] The presence of disordered layers above the crystalline monolayer could also inhibit the tilting of the molecules believed necessary to initiate the butane monolayer melting.[2] This would be consistent with the increase in the film's melting point observed at coverages of $\theta=2.2$ and 3.1 (see Fig. 5).

We have noted earlier that the leveling off in the low-Q diffuse intensity as well as in the bulk (051) peak intensity in the coverage range $2.5<\theta<3.4$ may correlate with bilayer crystallization. The second crystalline layer could be formed from disordered molecules already present in the second and third layers of the film or from those newly added. In either case, the amount of disordered butane in the cell would remain roughly constant during bilayer crystallization.

A linear increase in the low-Q diffuse intensity recommences at a coverage $\theta\approx3.4$ as does the intensity of the bulk (051) peak. However, the rate of increase for both is slower than for the coverage range $1.5<\theta<2.6$. It is not clear to us where this additional disordered material is accumulating after bilayer crystallization. Since it tracks the bulk growth, the diffuse intensity may be associated with disordered molecules, which accumulate at grain boundaries between bulk domains. We speculate that the slower growth rate of disordered material for $\theta>3.4$ may be related to the capillary condensation occurring at these coverages.[34]

E. Evidence for a wetting transition

At coverages of $\theta=2.2$ and 3.1, we have seen that both film and bulk Bragg peaks disappear between temperatures of 128 and 133 K. In their place, we observe a broader peak centered at $Q=1.5$ Å^{-1}, the position of the monolayer (20) reflection (see Fig. 5). There is some evidence of a second-order peak near 3 Å^{-1}, although it is largely obscured by the imperfect subtraction of the graphite background in that Q range. We interpret this behavior as indicating the melting of the crystalline monolayer ($\theta=2.2$) and of the bilayer crystal ($\theta=3.1$). Since the bulk Bragg peaks also disappear at both coverages by 133 K, i.e., below the bulk melting point at 135 K, we infer that a wetting transition has occurred so that only fluid film is present at temperatures above 133 K.

A possible structure of the film at 133 K, which we have considered for coverages $\theta=2.2$ and 3.1 is a smecticlike liquid-crystal phase induced by the rodlike shape of the molecule.[1,9,35] That is, the molecules remain nearly aligned along the **b** direction of the low-temperature crystalline phase [see Fig. 2(a)], although translational order along this direction is lost.[36] These rows of molecules, separated by a distance $a/2=4.26$ Å, would result in a broad diffraction peak centered at the monolayer (20) position.

F. Model for quasiepitaxial growth

Our discussion of the butane film structure in this section is summarized schematically by the model in Fig. 8. Growth of the crystalline monolayer is followed by adsorption of a disordered buffer layer, which allows bulk crystallites to grow with their (100) planes preferentially oriented parallel to the graphite surface [Fig. 8(a)]. During the growth of the disordered second layer and the early stages of bulk growth the monolayer is uniaxially compressed. To drive this compression, we have suggested that the disordered material continues to accumulate at the monolayer-bulk interface in this coverage range $(1.5<\theta<2.5)$.

As illustrated in Fig. 8(b), bilayer crystallization begins at a coverage $\theta\approx 2.5$ corresponding to the onset of the plateau in the amounts of bulk and disordered material [Figs. 4(a) and 4(b)]. The third layer of the film is partially occupied with disordered molecules at this point. This state persists in the coverage range $2.5<\theta<3.4$ with additional molecules either crystallizing in the second layer of the film or replenishing disordered molecules in the film which have crystallized.

Above a coverage $\theta\approx 3.4$, growth of preferentially ordered bulk and disordered material recommences, although at a slower rate than before bilayer crystallization. Bulk growth now includes capillary-condensed material. It is not clear whether disordered material continues to accumulate at the bulk-film interface or at grain boundaries of the polycrystalline bulk butane.

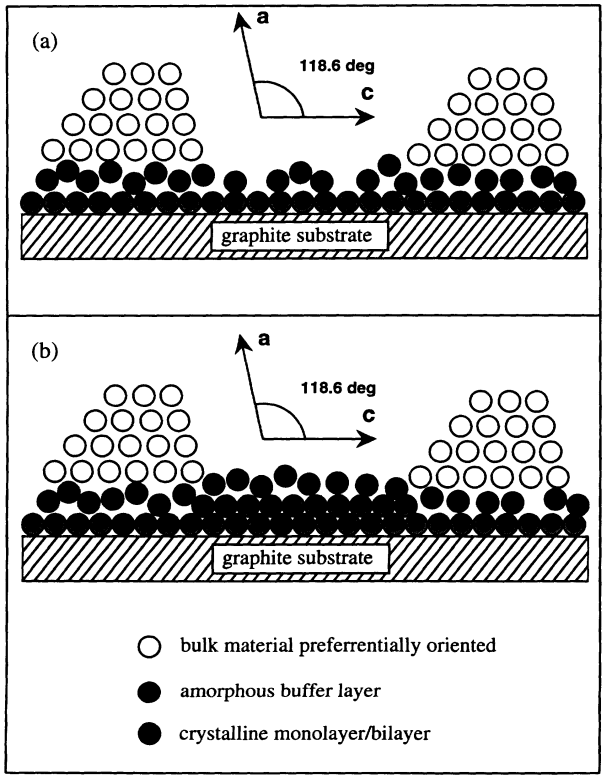

FIG. 8. Schematic model for the growth of butane films on the graphite basal-plane surface (a) coverage $\theta\approx 2$ and (b) coverage $\theta\approx 4$. Insets show lattice vectors for bulk butane.

The model in Fig. 8 can be described qualitatively as one of quasiepitaxial growth. Mismatch between the molecular orientations and lattice constants of the monolayer and those of the bulk is too great to allow growth of a multilayer crystalline film. We have suggested that a buffer region of disordered material at the monolayer-bulk interface mitigates the steric mismatch of the two phases allowing the initial growth of preferentially oriented bulk crystallites.

G. Comparison of the growth modes of butane and nitrogen on graphite

One might expect the structure of a film of a more spherical molecule such as nitrogen to depend less strongly on steric properties than does one of butane. Nevertheless, the two adsorbates have remarkably similarly growth modes on the graphite (0001) surface. The N_2 film structure has been investigated extensively by neutron diffraction up to coverages of ten layers.[15] Like butane, the uncompressed N_2 monolayer forms a rectangular unit cell with a two-sublattice HB structure. It differs from butane in that it is completely commensurate $(\sqrt{3}\times 3)$ with the graphite surface, whereas the butane monolayer is only commensurate in the $\sqrt{3}$ direction in this coverage range. Above monolayer completion, both the N_2 and the butane monolayers compress perpendicular to the $\sqrt{3}$ direction. In the case of N_2, the $\sim 3\%$ uniaxial compression out of registry is followed by a nearly isotropic compression to the so-called triangular incommensurate phase. The latter transition is complete at about 1.7 layers (in coverage units of the commensurate phase). We have seen that a coverage $\theta\geq 3$ is required for a 4% uniaxial compression of the butane film to a completely commensurate rectangular $(2\sqrt{3}\times 3)$ phase, and we have suggested that compression terminates upon completion of bilayer crystallization.

There are also similarities between the low-temperature structure of N_2 and butane films on graphite at higher coverages. Like butane, the N_2 neutron-diffraction patterns are consistent with disordered material adsorbing on the compressed crystalline monolayer.[15] Also, after a second and third layer of disordered material adsorb, the first two layers crystallize into a bilayer structure with some reorientation of the molecules in the first layer. The N_2 bilayer crystal is slightly less dense than the incommensurate compressed monolayer phase while there is a monotonic compression of the butane film from the partially commensurate monolayer to crystallization of the fully commensurate bilayer.

For both N_2 and butane adsorbed on graphite, there is a roughly linear growth of bulk material above a coverage $\theta\sim 3.7$ layers. In contrast to N_2, bulk growth of butane initially occurs at $\theta\approx 1.7$ before leveling off for coverages $2.6<\theta<3.8$. We are unsure of the reason for this difference. Possibly bulk growth is encouraged at a lower coverage for butane because there is better match of the bulk lattice constant to the monolayer than to the bilayer [see Figs. 2(c) and 4(c)]. Bulk growth temporarily ceases during bilayer crystallization and is reentrant when fur-

ther film growth becomes sterically unfavorable. When it resumes, there is growth of both preferentially oriented as well as capillary-condensed bulk particles.

A recent ellipsometry experiment by Volkmann and Knorr[37] found that, at temperatures below the α-β structural phase transition of bulk N_2, the vapor-film interface of N_2 adsorbed on a pyrolytic graphite (0001) surface remains optically smooth up to thicknesses of 40 layers. These authors propose that in this temperature range there is epitaxial growth of bulk N_2 above the crystalline bilayer. They suggest that the disordered third and fourth layers inferred by neutron diffraction[15] provide a buffer region to accommodate the lattice and molecular orientational mismatch between the crystalline bilayer and the epitaxial bulk α-N_2.[37]

This model for the growth of N_2 on graphite is quite similar to that which we propose for butane. A valuable check on the validity of this model for N_2 would be to analyze the neutron-diffraction patterns at high coverage[15] for preferential orientation of the bulk crystallites as we have done in the case of butane.

V. SUMMARY AND CONCLUSIONS

The growth of butane films on graphite has provided several surprises. The similarity of the monolayer structure to that of the (100) bulk plane does not lead to complete wetting of the film. Instead, a rather extreme case of incomplete wetting occurs in which only one or possibly two crystalline layers grow at low temperature prior to the nucleation of bulk clusters. However, the similarity of the monolayer and bulk structures results in a quasiepitaxial growth mode in which the bulk crystallites are preferentially oriented with respect to the graphite surface. The adsorption of disordered material above the crystalline monolayer appears to be necessary in providing a buffer region conducive to the growth of oriented bulk crystallites.

We were also surprised by the reentrant growth of the preferentially oriented bulk material, which occurs at coverages above bilayer crystallization. Although we have presented several arguments for capillary condensation not occurring at the lower coverages where bulk first appears, synchrotron x-ray diffraction experiments are planned with butane films adsorbed on single-crystal substrates in order to confirm this interpretation.

In addition, the similarity in the quasiepitaxial growth mode of the butane film to that of the more spherical N_2 molecule was unanticipated. It suggests that this growth mode may be common to other films of rod-shaped molecules for which the substrate binding is sufficiently strong. Indeed, electron-diffraction studies of thick ethane films on single-crystal graphite have also been interpreted in terms of oriented bulk crystallites.[38] Conditions favoring this quasiepitaxial growth mode would be the existence of a close-packed plane of the bulk phase to which the long axis of the molecules is nearly parallel as well as a good match between the monolayer and in-plane bulk lattice constants. Films of rod-shaped molecules having a larger aspect ratio than butane would seem to be likely candidates for such growth.

ACKNOWLEDGMENTS

We are indebted to A. D. Migone for providing us with the results of his heat capacity measurements prior to publication and for enlightening discussions of their interpretation. The authors would also like to thank F. Y. Hansen and G. S. Pawley for helpful discussions. In addition, B. Matthies provided valuable assistance in collecting and analyzing the data. This work was supported by the National Science Foundation under Grants Nos. DMR-9011069 and DMR-9314235, and the University of Missouri Research Reactor.

---

*Present address: Campus Computing, University of Missouri-Columbia, Columbia, MO 65211.

[1]H.Taub, in *The Time Domain Surface and Structural Dynamics,* Vol. 228 of *NATO Advanced Study Institute, Series C: Mathematical and Physical Sciences,* edited by G. J. Long and F. Grandjean (Kluwer, Dordrecht, 1988), p. 467.

[2]F. Y. Hansen and H. Taub, Phys. Rev. Lett. **69**, 652 (1992); F. Y. Hansen, J. C. Newton, and H. Taub, J. Chem. Phys. **98**, 4128 (1993); F. Y. Hansen and H. Taub, in *Phase Transitions in Surface Films 2,* Vol. 267 of *NATO Advanced Study Institute, Series B: Physics,* edited by H. Taub, G. Torzo, H. J. Lauter, and S. C. Fain, Jr. (Plenum, New York, 1991), p. 153.

[3]S. Grannick, Science **253**, 1374 (1991).

[4]G. B. Hess, in *Phase Transitions in Surface Films 2* (Ref. 2), p. 357.

[5]M. Bienfait, J. L.Seguin, J. Suzanne, E. Lerner, J. Krim, and J. G. Dash, Phys. Rev. B **29**, 983 (1984).

[6]R. J. Muirhead, J. G. Dash, and J. Krim, Phys. Rev. B **29**, 5074 (1984).

[7]F. T. Gittes and M. Schick, Phys. Rev. B **30**, 209 (1984).

[8]D. A. Huse, Phys. Rev. B **29**, 6985 (1984).

[9]J. C. Newton, Ph.D. thesis, University of Missouri–Columbia, 1989.

[10]K. Refson and G. S. Pawley, Acta Crystallogr. Sect. B **42**, 402 (1986).

[11]J. Z. Larese, Q. M. Zhang, L. Passell, J. M. Hastings, J. R. Dennison, and H. Taub, Phys. Rev. B **40**, 4271 (1989).

[12]G. J. Trott, Ph.D. thesis, University of Missouri–Columbia, 1981.

[13]G. J. Trott, H. Taub, F. Y. Hansen, and H. R. Danner, Chem. Phys. Lett. **78**, 504 (1981).

[14]R. Berliner, D. F. R. Mildner, J. Sudol, and H. Taub, in *Position Sensitive Detection of Thermal Neutrons,* edited by P. Convert and J. B. Forsyth (Academic, New York, 1983), p. 120.

[15]S.-K. Wang, J. C. Newton, R. Wang, H. Taub, J. R. Dennison, and H. Shechter, Phys. Rev. B **39**, 10 331 (1989).

[16]Manufactured by Le Carbone Lorraine, Departément Produits Spéciaux, 37 à 41 rue Jean Jaures, 92231 Gennevilliers, France.

[17]D. M. Small, in *Handbook of Lipid Research* (Plenum, New York, 1986), Vol. 4, p. 561.

[18]The pattern shown in Fig. 1 reproduced in two separate measurements. However, there is a small discrepancy between it

and the one obtained earlier in Refs. 12 and 13 in that the intensity ratio of the (11)–(20) peaks is somewhat smaller than obtained in the earlier work. While we are not certain of its origin, this discrepancy does not affect our conclusions on the validity of the HB structure described below.

[19]H. M. Rietveld, Acta Crystallogr. **22**, 151 (1967); J. Appl. Crystallogr. **2**, 65 (1969).

[20]A. E. Kitaigorodskii, *Molecular Crystals* (Academic, New York, 1973).

[21]It should be noted that even if there were not disordered butane in the cell, the incoherent scattering from both D and impurity H atoms would result in a small linear increase in the diffuse signal. However, the increase in the diffuse scattering at coverages $\theta \approx 1.5$ and its leveling off in the range $2.5 \leq \theta \leq 3.4$ are inconsistent with attributing all of the diffuse intensity to incoherent scattering from the D and H atoms.

[22]M. T. Alkhafaji and A. D. Migone, Phys. Rev. B **48**, 1761 (1993).

[23]A. D. Migone (private communication).

[24]J. Krim, J. Suzanne, H. Shechter, R. Wang, and H. Taub, Surf. Sci. **162**, 446 (1985).

[25]Presumably, the uniaxial compression is also driven by the lateral forces favoring commensurability along the **b** direction.

[26]The difference pattern in Fig. 6 will also contain a smaller contribution from disordered material, which appears in the cell at coverages $\theta \geq 3.4$ [see Fig. 4(b)].

[27]A. C. Larson and R. B. Von Dreele (unpublished).

[28]J. K. Kjems, L. Passell, H. Taub, J. G. Dash, and A. D. Novaco, Phys. Rev. B **13**, 1446 (1976).

[29]W. A. Dollase, J. Appl. Crystallogr. **19**, 267 (1986).

[30]A. March, Z. Kristallogr. Kristallgeom. Krystallphys. Kristallchem. **81**, 285 (1932).

[31]J. G. Aston and G. H. Messerly, J. Am. Chem. Soc. **62**, 1917 (1940).

[32]The broadening is most apparent for the bulk peaks near $Q = 1.5$ Å^{-1} in the difference patterns at coverages of $\theta = 3.1$ and 2.2 [Figs. 7(d) and 7(e), respectively]. The fact that we observe bulk peaks at a coverage as low as $\theta = 2.2$ implies that the interfacial contact area of the bulk particles with the monolayer is small compared to the total monolayer area. We estimate a bulk particle dimension of ~ 50 Å from the width of the (031) peak in the $\theta = 6.0$ diffraction pattern in Fig. 3.

[33]K. Morishige, K. Kawamura, M. Yamamoto, and I. Ohfuji, Langmuir **6**, 1417 (1990).

[34]For example, the bulk crystallite size in the capillary-condensed material might be constrained by morphological features of the graphite substrate such as pore diameters or particle sizes and shapes. As the amount of capillary-condensed butane grows, disordered material would accumulate at the grain boundaries between bulk crystallites, but at a slower rate than it did initially at the monolayer-bulk interface.

[35]K. Morishige, N. Kawai, and M. Shimizu, Phys. Rev. Lett. **70**, 3904 (1993).

[36]For a rectangular monolayer unit cell commensurate with the graphite surface in the **a** direction, the **b** lattice vector would lie parallel to a line connecting centers of adjacent carbon hexagons in the graphite basal plane. Calculations in Ref. 12 indicate that "troughs" in the molecule-substrate potential lie in this direction. These may tend to align the butane molecules.

[37]U. G. Volkmann, and K. Knorr, Phys. Rev. Lett. **66**, 473 (1991).

[38]J-M. Gay, J. Suzanne, G. Pepe, and T. Meichel, Surf. Sci. **204**, 69 (1988).

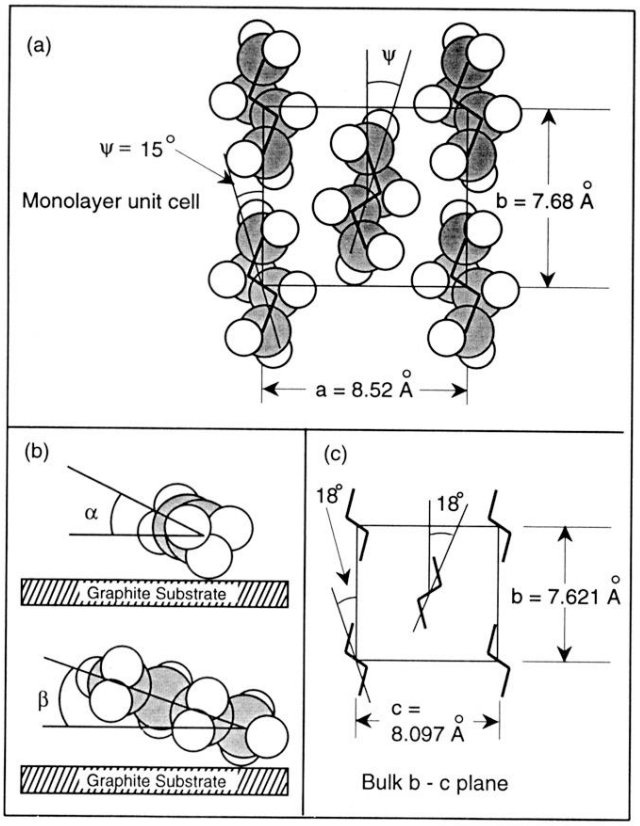

FIG. 2. Models of the monolayer and bulk butane structures. (a) Projection of the HB monolayer structure on the graphite (0001) surface. For clarity, the van der Waals radii of individual atoms have been reduced by approximately 50%. (b) Diagrams defining the out-of-plane orientational parameters α and β: view along the long axis of the molecule (top panel) and perpendicular to the long axis (lower panel). (c) Projection of the low-temperature monoclinic structure of bulk butane on the (100) plane. The carbon skeleton of the butane molecules is represented by a thick solid line.

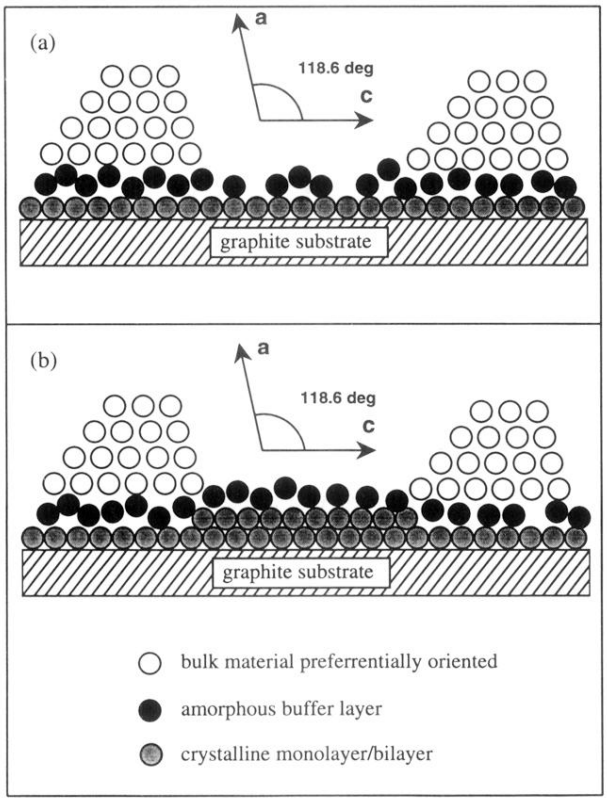

FIG. 8. Schematic model for the growth of butane films on the graphite basal-plane surface (a) coverage $\theta \approx 2$ and (b) coverage $\theta \approx 4$. Insets show lattice vectors for bulk butane.